Explicit Generalized Predictive Algorithms for Speed Control of PMSM Drives

Fast Explicit Form with Field Weakening and Current Limitation

Květoslav Belda
Department of Adaptive Systems
Institute of Information Theory and Automation of ASCR
Pod Vodárenskou věží 4, 182 08 Prague 8, Czech Republic
e-mail: belda@utia.cas.cz

David Vošmik
Regional Innovation Centre for Electrical Engineering (RICE)
University of West Bohemia (UWB)
Univerzitní 26, 306 14 Pilsen, Czech Republic
e-mail: vosmik1@rice.zcu.cz

***Abstract*-The paper deals with Generalized Predictive Control algorithms applied to the electric drives employing Permanent Magnet Synchronous Motors (PMSM). The Generalized Predictive Control (GPC) belongs to the multi-step model-based control design. The presented GPC algorithms are arranged in a specific explicit form for direct application in PMSM drives. The algorithms are supplemented with two front-end modules, which enable GPC algorithms to solve tasks of field weakening and current limitation. The design and implementation of proposed explicit GPC solution including modules are explained in the paper. The solution was experimentally verified at a speed control task. Performed experiments are documented by the time histories in oscillogram screenshots and figures.**

Keywords — PMSM drives; speed control; field weakening; current limitation; Generalized Predictive Control.

I. INTRODUCTION

Nowadays, advanced types of electrical drives are based on 3-phase Permanent Magnet Synchronous Motors (PMSM). Due to few mechanical elements leading to long operation life with minor demands on maintenance, those motors have great potential in wide range of applications in traffics, robotics and mechatronics in general.

From control point of view, the PMSM require to control simultaneously amplitude and frequency of all three terminal Alternate Currents (AC) in Pulse-Width-Modulation (PWM). Input to the PWM is amplitude and phase of stator voltage. Those values are generated by control algorithms. Usual solution is based on PI controllers coupled in cascade loops [4]. That cascade configuration represents set of autonomous PI controllers, where mutual relations mean external disturbances. The setting of PI controllers is limited only on several static constants. Their fixed configuration does not give any space for some possible improvements or e.g. modifications solving further control requirements. The configuration drawbacks consist especially in the behavior in limit or changeable states and in constant controller setting without any adaptation. It causes that cascade control, due to essentially limited bandwidth, can be prone to violation in dynamic applications [3].

This paper deals with methods of a model-based approach, specifically with a model-based Generalized Predictive Control (GPC) [2], which represents a popular way due to its flexibility and clarity. It can naturally consider all available pieces of information from a mathematical model and user requirement in a control design within one optimization task [4], [5]. The GPC or its computation procedures can be formulated as a multi-objective optimization involving different control targets [1], [2].

The paper follows from previous works of authors [4], [6], in which the design principles of GPC algorithms to PMSM were introduced. The contribution of this paper consists in novel addressing of the field weakening and current limitation problems [10] and in novel GPC algorithms in a specific explicit form suitable for direct use in real PMSM drive applications. The proposed algorithms differ in the number of involved integrators (one or two) suppressing control offset [7], [8]. The explicit form employs fixed control laws, gains of which are pre-computed off-line for a specific range of motor speed (electrical rotor speed). The proposed explicit algorithms are supplemented with two front-end modules suitably adapting algorithm input signals. The modules due to a signal adaptation enable GPC to solve field weakening and current limitation subtasks. The both modules and appropriate GPC algorithm form one compact generalized predictive controller. Developed GPC algorithms as controllers were experimentally verified at a speed control task [1], [9]. Performed experiments are documented by the time histories illustrated in oscillogram screenshots and figures.

The organization of the paper is as follows. Section II. outlines a suitable mathematical model for model-based control design. Section III. introduces basic schemes of predictive control, including field weakening and current limitation modules, and standard vector PI control for comparison. Section IV. focuses on the principles of GPC algorithms and Section V. clarifies solution of field weakening and current limitation within GPC design. Finally, Section VI. shows data from real experiments for both proposed GPC algorithms.

978-1-4799-0223-1/13/$31.00 ©2013 IEEE

II. MATHEMATICAL MODEL FOR CONTROL DESIGN

A suitable mathematical model for a control design follows from the voltage distribution in individual phases of three AC phase system and from torque equilibrium equation. The model of PMSM (using Clarke and Parke transformations) is defined by the following set of the equations (1) - (3) in d-q rotating field coordinate system or rotating reference frame:

$$u_{Sd} = R_S\, i_{Sd} + L_d \frac{d}{dt} i_{Sd} - L_q\, \omega_e\, i_{Sq} \tag{1}$$

$$u_{Sq} = R_S\, i_{Sq} + L_q \frac{d}{dt} i_{Sq} + L_d\, \omega_e\, i_{Sd} + \psi_M\, \omega_e \tag{2}$$

where R_S, $L_{d,q}$, ($=L_S$ for surface PM) and ψ_M are motor parameters (see TABLE I.), u_{Sd}, u_{Sq} are d-q voltages (system inputs), $i_{Sd,\,Sq}$ are d-q currents, ω_e is the electrical rotor speed (mechanical speed $\omega_m = \omega_e / p$; p is a number of pole pairs),

$$J\ddot{\vartheta}_e = \frac{3}{2} p^2 \psi_M\, i_{Sq} - B\omega_e - p\tau_L \tag{3}$$

where J, B are other motor parameters (see TABLE I.), ϑ_e is the electrical rotor position, τ_L is a load torque.

The model (1) - (3) can be rearranged in a state-space like form [4], (for used motor: $L_d = L_q = L_S$; i.e. surface PMSM):

$$\frac{d}{dt}\begin{bmatrix} i_{Sd} \\ i_{Sq} \\ \omega_e \\ \tau_L \end{bmatrix} = \begin{bmatrix} -\frac{R_S}{L_S} & \omega_e & 0 & 0 \\ -\omega_e & -\frac{R_S}{L_S} & -\frac{\psi_M}{L_S} & 0 \\ 0 & \frac{3}{2}\frac{p^2}{J}\psi_M & -\frac{B}{J} & -\frac{p}{J} \\ 0 & 0 & 0 & 0 \end{bmatrix} \begin{bmatrix} i_{Sd} \\ i_{Sq} \\ \omega_e \\ \tau_L \end{bmatrix} + \begin{bmatrix} \frac{1}{L_S} & 0 \\ 0 & \frac{1}{L_S} \\ 0 & 0 \\ 0 & 0 \end{bmatrix} \begin{bmatrix} u_{Sd} \\ u_{Sq} \end{bmatrix} \tag{4}$$

$$\frac{d}{dt}\mathbf{x}(t) = \mathbf{A}_C(\omega_e)\,\mathbf{x}(t) + \mathbf{B}_C\,\mathbf{u}(t) \tag{5}$$

where $\mathbf{A}_C(\omega_e)$ is a variable state-space matrix relative to ω_e, $\mathbf{B}_C$ is a constant input matrix. The two nonlinear terms $\omega_e\, i_{Sq}$ and $\omega_e\, i_{Sd}$ in (1) and (2) are decomposed in (4) according to the idea of a specific linearizing decomposition described in [6]. The state-space model (4) or (5) represents suitable form for model-based control design.

III. BASIC CONROL SCHEMES

In this section, the differences of standard cascade vector PI control scheme and GPC scheme are introduced. The schemes are intended for speed control task, $\omega_e \to \omega_{ew}$; $i_{Sd}, i_{Sq} \to \min$.

The cascade control approach consists of fourth separate PI controllers (Fig. 1). In contrast, the predictive control is represented only by one GPC controller block, which is preceded by two input-adapting modules of field weakening FW$_M$ and current limitation CL$_M$ (Fig. 2).

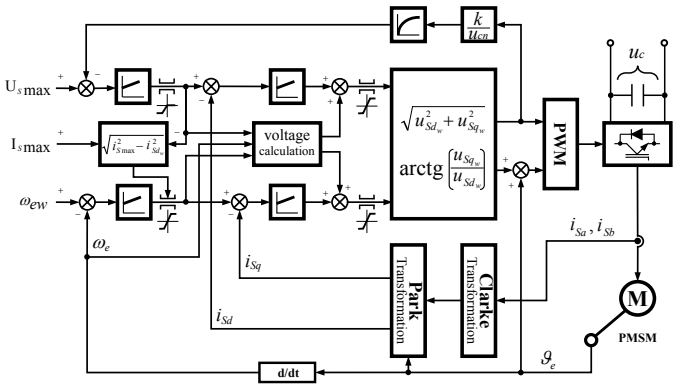

Fig. 1. Standard control scheme of cascade vector PI control.

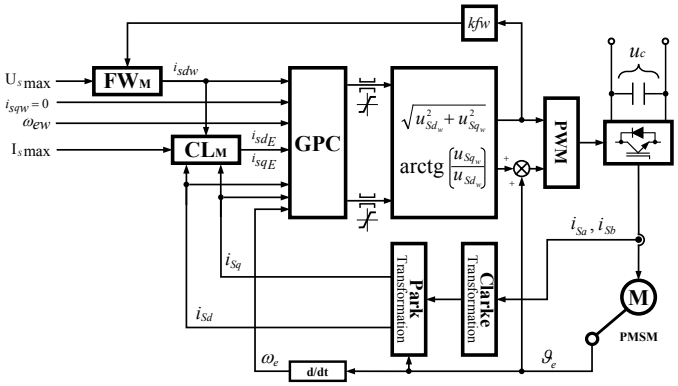

Fig. 2. Primary control scheme of Generalized Predictive Control.

In the scheme of PI control in Fig. 1, the controllers interact without any optimization. In GPC scheme in Fig. 2, the control action computation is performed only in one compact block. This block covers one lumped complex optimization for all user control requirements, i.e. required reference signals:

- electrical rotor speed ω_{ew}
- field weakening ($\omega_e \uparrow\uparrow \to i_{Sdw} \neq 0;\ 0 < \| i_{Sdw} \| < \mathrm{I}_s\mathrm{max}$)
- current limitation $\sqrt{i_{Sd}^2 + i_{Sq}^2} \leq \mathrm{I}_s\mathrm{max}$

The optimization procedure is based on specific evaluation of one criterion cost function. The principle of the design and computation of control actions will be explained in next section.

The modules FW$_M$ and CL$_M$ form a simple extension or suitable input adaptation for GPC design. The module FW$_M$ follows usual procedure of the field weakening. However, the module CL$_M$, adapting currents for their limitation, is developed with features of predictive control parameters. The both modules will be described in Section V.

IV. PREDICTIVE CONTROL ALGORITHMS

The ***GPC algorithms*** are usually implemented as discrete (digital) procedures [2], which provide computation of control actions within one optimization calculation. In general, the calculation employs predictions of expected future output values mathematically defined by equations of predictions. Those equations are closely related to the form of a cost function. At a predictive control design, the quadratic cost function is used. Its form may be various. It depends on used equations of predictions or control targets. In this paper, two specific GPC algorithms are considered. They differ in the number of included integrators. Their features will be obvious from experiments. They are expressed in a compact matrix notation.

• ***1st GPC algorithm*:** The cost function form is as follows [4]

$$J_k = \| \mathbf{Q}_{\mathrm{yw}} (\hat{\mathbf{y}} - \mathbf{w}) \|^2 + \| \mathbf{Q}_{\Delta \mathrm{y}} \Delta \hat{\mathbf{y}} \|^2 + \| \mathbf{Q}_{\Delta \mathbf{u}} \Delta \mathbf{u} \|^2 \qquad (6)$$

Optimization of this function leads to the *1st GPC algorithm with one integrator* (single integration – I. integrator):

$$\begin{aligned} \Delta \mathbf{u}_k = \mathbf{M} \, & (\mathbf{G}_2^T \, \mathbf{Q}_{\mathrm{yw}} \, \mathbf{G}_2 + \mathbf{G}_1^T \, \mathbf{Q}_{\Delta \mathrm{y}} \, \mathbf{G}_1 + \mathbf{Q}_{\Delta \mathbf{u}})^{-1} \\ & \times (\, \mathbf{G}_2^T \, \mathbf{Q}_{\mathrm{yw}} (\mathbf{I} \, \mathbf{y}_k + \mathbf{f}_2 \, \Delta \mathbf{x}_k - \mathbf{w}) + \mathbf{G}_1^T \, \mathbf{Q}_{\Delta \mathrm{y}} (\mathbf{f}_1 \, \Delta \mathbf{x}_k) \,) \end{aligned} \qquad (7)$$

where a rectangular matrix $\mathbf{M}$ serves for row selection corresponding to control actions in time-instant k. The formula (7) can be reshaped to the form of control law (8):

$$\begin{aligned} \mathbf{e}_k &= \mathbf{w}_k - \mathbf{y}_k \\ \Delta \mathbf{u}_k &= \mathbf{K}_{\mathrm{e}} \, \mathbf{e}_k - \mathbf{K}_{d\mathbf{x}} \, \Delta \mathbf{x}_k \\ \mathbf{u}_k &= \mathbf{u}_{k-1} + \Delta \mathbf{u}_k \end{aligned} \qquad (8)$$

The quadratic function (6) and control actions $\Delta \mathbf{u}_k$ (7) or gains $\mathbf{K}_{\mathrm{e}}$ and $\mathbf{K}_{d\mathbf{x}}$ in control law (8) exploit the following equations of predictions involving output equation $\mathbf{y}_k = \mathbf{C} \, \mathbf{x}_k$:

$$\begin{aligned} \Delta \hat{\mathbf{y}} &= \mathbf{f}_1 \, \Delta \mathbf{x}_k + \mathbf{G}_1 \, \Delta \mathbf{u} \\ \hat{\mathbf{y}} &= \mathbf{I} \, \mathbf{y}_k + \mathbf{f}_2 \, \Delta \mathbf{x}_k + \mathbf{G}_2 \, \Delta \mathbf{u} \end{aligned} \qquad (9)$$

where matrices $\mathbf{f}_1$ and $\mathbf{G}_1$ are defined as follows

$$\mathbf{f}_1 = \begin{bmatrix} \mathbf{CA} \\ \vdots \\ \mathbf{CA}^N \end{bmatrix}, \qquad \mathbf{G}_1 = \begin{bmatrix} \mathbf{C} & & \mathbf{B} \cdots & \mathbf{0} \\ & \vdots & \ddots & \vdots \\ \mathbf{C} \, \mathbf{A}^{N-1} \, \mathbf{B} & \cdots & \mathbf{CB} & \end{bmatrix} \qquad (10)$$

and $\mathbf{f}_2$ and $\mathbf{G}_2$ are similar, only their each element includes the element from row above, as indicated in (11)

$$\mathbf{f}_2 = \begin{bmatrix} \mathbf{CA} \\ \mathbf{CA} + \mathbf{CA}^2 \\ \mathbf{CA} + \mathbf{CA}^2 + \mathbf{CA}^3 \\ \vdots \end{bmatrix}, \quad \mathbf{G}_2 = \begin{bmatrix} & & \mathbf{CB} & \mathbf{0} & \cdots \\ & & \mathbf{CB} + \mathbf{CAB} & \mathbf{CB} & \ddots \\ & & \mathbf{CB} + \mathbf{CAB} + \mathbf{CA}^2\mathbf{B} & & \ddots \\ & & \vdots & \vdots & \ddots \end{bmatrix} \qquad (11)$$

• ***2nd GPC algorithm*:** The cost function form is considered in the following way

$$J_k = \| \mathbf{Q}_{\mathrm{yw}} (\hat{\mathbf{y}} - \mathbf{w} - \hat{\mathbf{e}}) \|^2 + \| \mathbf{Q}_{\Delta \mathrm{y}} \Delta \hat{\mathbf{y}} \|^2 + \| \mathbf{Q}_{\Delta \mathbf{u}} \Delta \mathbf{u} \|^2 \qquad (12)$$

where predictions of particular $\hat{\mathbf{y}}_j$ are defined as follows:

$$\begin{aligned} \hat{\mathbf{y}}_j &= \mathbf{y}_k + \sum_{i=k+1}^{j} \Delta \hat{\mathbf{y}}_i, \quad j = k+1, k+2, \cdots, k+N \\ \hat{\mathbf{y}} &= [\, \hat{\mathbf{y}}_{k+1}, \quad \hat{\mathbf{y}}_{k+2}, \quad \cdots \quad \hat{\mathbf{y}}_{k+N} \,]^T \end{aligned} \qquad (13)$$

Optimization of function (12) leads to the *2nd GPC algorithm with two integrators* (double integration):

$$\begin{aligned} \Delta \mathbf{u}_k = \mathbf{M} \, & ((\mathbf{G}_2 + \mathbf{G}_3)^T \, \mathbf{Q}_{\mathrm{yw}} \, (\mathbf{G}_2 + \mathbf{G}_3) + \mathbf{G}_1^T \, \mathbf{Q}_{\Delta \mathrm{y}} \, \mathbf{G}_1 + \mathbf{Q}_{\Delta \mathbf{u}})^{-1} \\ & \times \big\{ (\mathbf{G}_2 + \mathbf{G}_3)^T \, \mathbf{Q}_{\mathrm{yw}} ((\mathbf{I} + \mathbf{f}_0) \, \mathbf{y}_k \\ & + (\mathbf{f}_2 + \mathbf{f}_3) \, \Delta \mathbf{x}_k - \mathbf{I} \, \bar{\mathbf{e}}_k - \mathbf{w} - \mathbf{w}_S) + \mathbf{G}_1^T \, \mathbf{Q}_{\Delta \mathrm{y}} (\mathbf{f}_1 \, \Delta \mathbf{x}_k) \big\} \end{aligned} \qquad (14)$$

which is transformed to the form of control law and complemented by equations of topical control error $\mathbf{e}_k$, its cumulative value $\bar{\mathbf{e}}_k$ (I. integrator) and equation for control actions $\mathbf{u}_k$ from their increments (II. Integrator) as follows

$$\begin{aligned} \mathbf{e}_k &= \mathbf{w}_k - \mathbf{y}_k \\ \bar{\mathbf{e}}_k &= \bar{\mathbf{e}}_{k-1} + \mathbf{e}_k \\ \Delta \mathbf{u}_k &= \mathbf{K}_{\bar{\mathrm{e}}} \, \bar{\mathbf{e}}_k + \mathbf{K}_{\mathrm{W}} \, \mathbf{w} + \mathbf{K}_{\mathrm{W}_S} \, \mathbf{w}_S \\ & \quad - \mathbf{K}_{\mathrm{y}_k} \, \mathbf{y}_k - \mathbf{K}_{d\mathbf{x}} \, \Delta \mathbf{x}_k \\ \mathbf{u}_k &= \mathbf{u}_{k-1} + \Delta \mathbf{u}_k \end{aligned} \qquad (15)$$

The quadratic function (12), expression of control actions $\Delta \mathbf{u}_k$ (14), and determined control gains $\mathbf{K}_{\mathrm{e}}$ and $\mathbf{K}_{d\mathbf{x}}$ in (15), arise from the following proposed equations of predictions:

$$\begin{aligned} \Delta \hat{\mathbf{y}} &= \mathbf{f}_1 \, \Delta \mathbf{x}_k + \mathbf{G}_1 \, \Delta \mathbf{u} \\ \hat{\mathbf{y}} &= \mathbf{I} \, \mathbf{y}_k + \mathbf{f}_2 \, \Delta \mathbf{x}_k + \mathbf{G}_2 \, \Delta \mathbf{u} \\ \hat{\mathbf{e}} &= \mathbf{I} \, \mathbf{e}_k + \mathbf{f}_0 \, \mathbf{y}_k + \mathbf{f}_3 \, \Delta \mathbf{x}_k + \mathbf{G}_3 \, \Delta \mathbf{u} \end{aligned} \qquad (16)$$

where matrices $\mathbf{f}_1$ and $\mathbf{G}_1$; and $\mathbf{f}_2$ and $\mathbf{G}_2$ are identical with their previous definitions. The matrices $\mathbf{f}_3$ and $\mathbf{G}_3$ are defined by analogy as indicated in (17)

$$\mathbf{f}_3 = \begin{bmatrix} \mathbf{0} \\ \mathbf{CA} \\ 2\mathbf{CA} + \mathbf{CA}^2 \\ \vdots \end{bmatrix}, \quad \mathbf{G}_3 = \begin{bmatrix} & & \mathbf{0} & \mathbf{0} & \cdots & \mathbf{0} \\ & & \mathbf{CB} & & \ddots & \vdots \\ & & 2\mathbf{CB} + \mathbf{CAB} & \ddots & & \mathbf{0} \\ & & \vdots & \ddots & \mathbf{CB} & \mathbf{0} \end{bmatrix} \qquad (17)$$

For the considered speed control task, the GPC or proposed algorithms in this section replace the conventional cascade structure by one numerical calculation.

Note finally that the GPC algorithms are implemented as discrete (digital) procedures. Therefore, due to linearized model form, the model (5) is the earliest discretized by usual way to the form:

$$\mathbf{x}_{k+1} = \mathbf{A}_k\ \mathbf{x}_k + \mathbf{B}\,\mathbf{u}_k\,, \qquad \mathbf{y}_k = \mathbf{C}\,\mathbf{x}_k \tag{18}$$

V. Front-End Modules of GPC

In terminal situations, the physical limits are crucial [10]. They must be considered in GPC design. The GPC generates control, which corresponds to the ideal situation with no limits and constrains. The constraints and modifications are usually solved in GPC design via quadratic programming [2]. That is a time-consuming procedure unsuitable for a fast real-time control of PMSM drives. The following two subsections propose simple fast solution tailored to PMSM keeping explicit form of GPC explained in the previous section.

A. Field Weakening Module - FW_M

If further increase of rotor speed is required and supply voltage cannot be appropriately increased too, just due to voltage supply limits, then the field weakening is necessary. Since the direct control of magnetic flux is not possible with respect to permanent magnets, the field weakening is provided by incorporating a negative d - component of current i_S.

That is the usual way, which requires meeting the following condition:

$$i_S = \sqrt{i_{Sd}^2 + i_{Sq}^2} \le \mathrm{I}_S\mathrm{max} \tag{19}$$

where $\mathrm{I}_S\mathrm{max}$ is admissible maximum stator current. The standard realization within control scheme is seen in Fig. 1.

The described idea of the field weakening can be used also in GPC design. However, the value of i_{Sd} represents new specific reference value i_{Sdw} being negative if weakening is necessary, otherwise being zero. This is the core of a Filed Weakening Module FW_M in front of GPC block – see Fig. 2. The module FW_M algorithm is expressed as follows:

$$\begin{aligned}
&u_S := \sqrt{u_{Sd}^2 + u_{Sq}^2}\ ;\\
&\textit{if}\ u_S \ge U_S\mathrm{max},\\
&\quad i_{Sdw} := (U_S\mathrm{max} - u_S)\,k_{fw}\ ;\\
&\quad \textit{if}\ \|\,i_{Sdw}\,\| > \mathrm{I}_S\mathrm{max},\ \ i_{Sdw} := -\,\mathrm{I}_S\mathrm{max}\ k_{i_{ub}}\ ;\ \textit{end}\\
&\textit{else}\\
&\quad i_{Sdw} := 0\ ;\\
&\textit{end}
\end{aligned} \tag{20}$$

where $U_S\mathrm{max}$ is admissible maximum stator voltage, k_{fw} is a field weakening gain and $k_{i_{ub}}$ is a margin coefficient. The gain k_{fw} suppresses the chattering in transition states, the coefficient $k_{i_{ub}}$ serves for keeping a space for current i_{Sq}.

B. Current Limitation Module - CL_M

The current limitation is key issue of every control design of PMSM drives. The current sum may not exceed admissible stator current $\mathrm{I}_S\mathrm{max}$, otherwise current overshoot can cause a drive malfunction or activation of current breakers leading to an undesirable drive operation interruption. The following algorithm of a Current Limitation Module CL_M (see Fig. 2) 'multiplies' the magnitudes of current d-q components so that to be reflected in the appropriate cost function during its optimization in GPC design.

$$\begin{aligned}
&i_{SdE} := i_{Sd}\ ;\\
&i_{SqE} := i_{Sq}\ ;\\
&\textit{if}\ \|\,i_{Sq}\,\| \ge \sqrt{\mathrm{I}_S^2\mathrm{max} - i_{Sdw}^2}\ ,\quad i_{SqE} := \left(\frac{\|\,i_{Sq}\,\|}{\mathrm{I}_S\mathrm{max}}\right)^{k_{sp}} i_{Sq}\ ;\\
&\textit{elseif}\ \|\,i_{Sd}\,\| > \mathrm{I}_S\mathrm{max}\ k_{i_{ub}}\ ,\quad i_{SdE} := \left(\frac{\|\,i_{Sd}\,\|}{\mathrm{I}_S\mathrm{max}}\right)^{k_{sp}} i_{Sd}\ ;\\
&\textit{end}
\end{aligned} \tag{21}$$

where k_{sp} is suitable selected exponent; and currents i_{SdE} and i_{SqE} are modified absolute inputs of GPC. Outlined algorithm causes that the appropriate real current components will be intensively suppressed by weighting matrices $\mathbf{Q}_{\mathbf{yw}}$ in appropriate cost function (6) or (12). Therefore, artificial proportional extension of appropriate current component appears as a big outlier against other terms in the criterion and optimization predominantly suppresses this outlier. From a practical point of view, the changeable lower limit $\sqrt{(\mathrm{I}_S^2\mathrm{max} - i_{Sdw}^2)}$ in (21) is reasonable to be held above some meaningful level so that the condition will be feasible.

Note, finally, that this solution gives acceptable results. However, it is not represent hard limitation, but only soft limitation, which comes close to hard limitation. From GPC design point of view, the proposed algorithm (21) does not change control design or tuning of control parameters, it only modifies selected inputs to the GPC controller.

VI. Hardware Implementation and Experiments

The algorithms were implemented in the control system developed at University of West Bohemia. The system is based on DSP TMS320f28335. This DSP works with floating point arithmetic and single precision format. The control system is connected to the laboratory PMSM drive of rated power 10.7 kW. The drive parameters are listed in the Table I. The testing stand with PMSM drive is shown in Fig. 6.

The individual gains of GPC are realized as functional approximation with parameter ω_e (analogy with [4]): $\mathbf{K}_{\mathbf{e}}(\omega_e)$, $\mathbf{K}_{d\mathbf{x}}(\omega_e)$ for the 1st algorithm and gains $\mathbf{K}_{\bar{\mathbf{e}}}(\omega_e)$, $\mathbf{K}_{\mathbf{W}}(\omega_e)$ $\mathbf{K}_{\mathbf{W}_S}(\omega_e)$, $\mathbf{K}_{\mathbf{y}_k}(\omega_e)$, $\mathbf{K}_{d\,\mathbf{x}}(\omega_e)$ for the 2nd GPC algorithm. The gains are selected on-line from the approximation. Thus, the computation of appropriate control actions by explicit control laws (8) or (15), supplemented by FW_M and CL_M modules, is fast and usable for real-time control of PMSM drives.

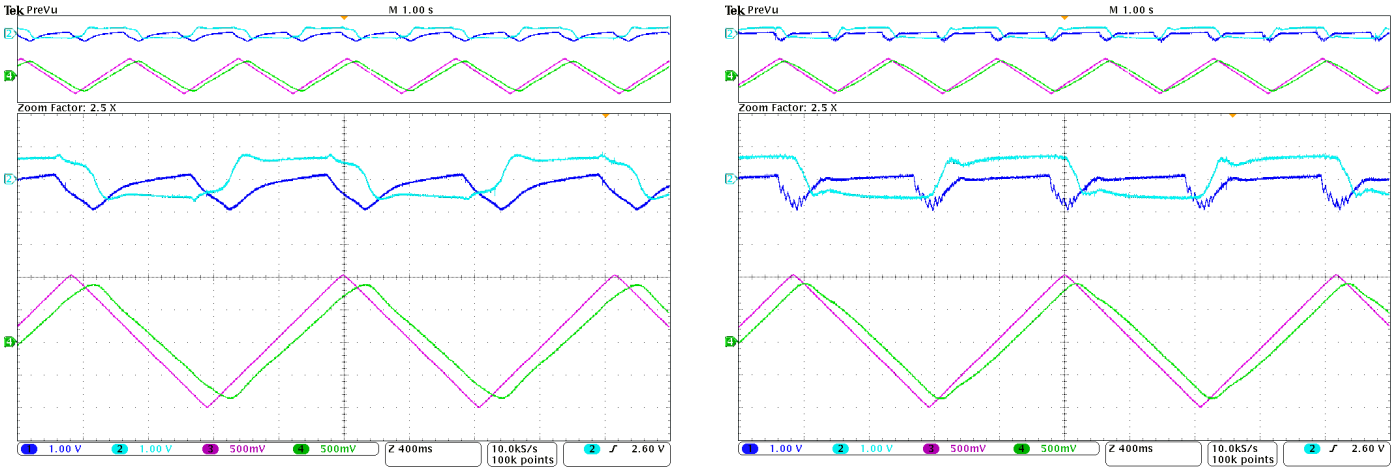

Fig. 3. GPC: comparison of 1st algorithm (left) and 2nd algorithm (right) for high triangular command speed signal; command speed ± 2000 rpm; ch1: i_{Sd} current (25A/1V), ch2: i_{Sq} current (25A/1V), ch3: command el. rotor speed (135Hz/1V), ch4: measured el. rotor speed (135Hz/1V).

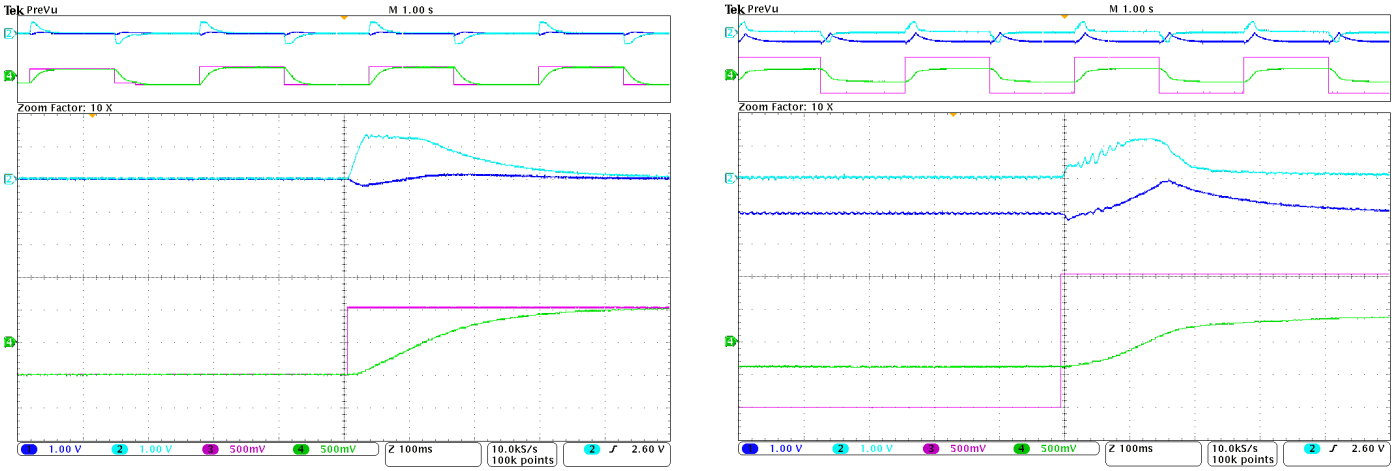

Fig. 4. GPC: current limitation and field weakening by 1st algorithm for supply voltage – Uc = 200V (left), Uc = 70V (right) and step signal; command speed ± 1000 rpm; ch1: i_{Sd} current (25A/1V), ch2: i_{Sq} current (25A/1V), ch3: command el. rotor speed (135Hz/1V), ch4: measured el. rotor speed (135Hz/1V).

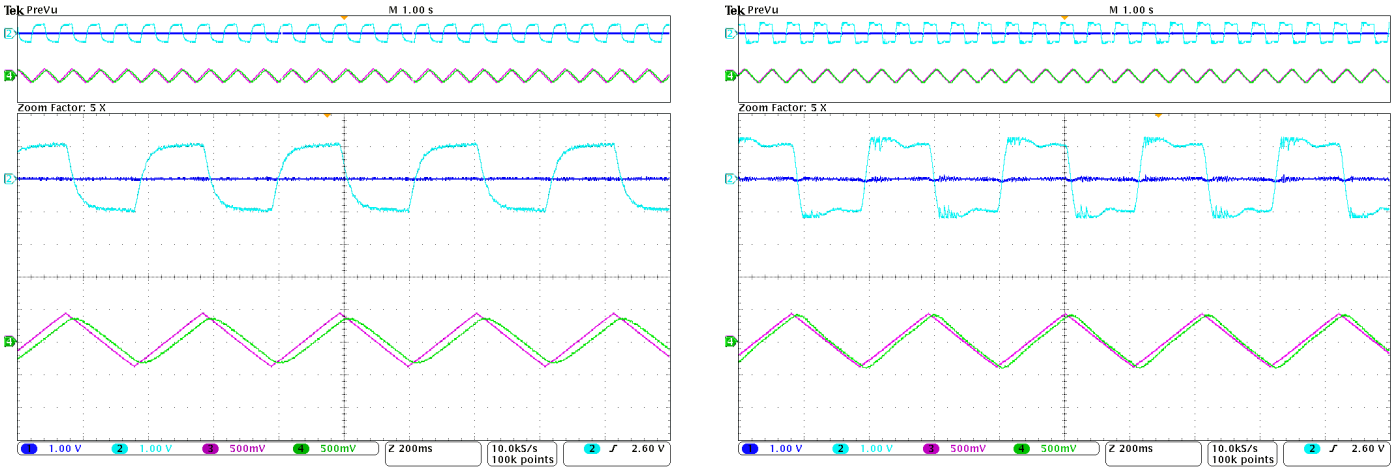

Fig. 5. GPC: comparison of 1st algorithm (left) and 2nd algorithm (right) for fast low triangular command speed signal; command speed ± 800 rpm; ch1: i_{Sd} current (25A/1V), ch2: i_{Sq} current (25A/1V), ch3: command el. rotor speed (135Hz/1V), ch4: measured el. rotor speed (135Hz/1V).

Experiments were realized for high triangular speed reference signal (ramp slope 4080 rpm/s), rectangular (step) signal and for fast low triangular signal (ramp slope 8000 rpm/s). The experiments are demonstrated by time histories of the state variables (i_{Sd}, i_{Sq}, $\omega_e = 2\pi pn/60$) of both GPC algorithms: 1st - single integration, 2nd - double integration.

Parameters of GPC are in TABLE II. and TABLE III. for Fig. 3 and Fig. 4 in the column "Value (A)" and for Fig. 5 in the column "Value (B)".

Fig. 3 demonstrates both algorithms when triangular speed profile is required. Speed reference profile passes through field weakening region bounded approx. by 900 rpm. The both GPC algorithms ensure reliable function in full speed operating range with similar behavior as standard cascade vector control [4]. The 1st algorithm slowly drifts from the reference slope. It is caused by only one integrator in the control circuit or control algorithm. The 2nd algorithm follows the ramp segments more closely owing to double integrator.

In Fig. 4, there are details of a behavior of the 1st algorithm specifically for two selected admissible levels of DC voltage at step speed reference signal. In the left subfigure, the current limitation of the i_{Sq} is obvious. The input DC terminal voltage was 200V. This powerful limitation is achieved by front-end CL$_M$ module (see subsection V.-B.). The limitation depends on the selection of specific coefficient-exponent k_{sp}. The proposed solution proves hard limitation character. However, respecting the principle exploiting features of control parameters of GPC (cost function weight, penalization $\mathbf{Q}_{yw}$), the limitation represents soft constraint approaching closely hard constraint only. In the right subfigure, the behavior for low supply voltage (only 70V) is shown. In that subfigure, it is clear, that the algorithm cannot reach required speed profile. Thus, the tested drive is deeply in field weakening region and torque part of current vector is very restricted to meet the maximum current limitation. The presented transient response demonstrates that the proposed algorithm can operate the drive in field weakening region appropriately as well.

Finally, the Fig. 5 shows both proposed GPC algorithms at fast low triangular speed reference signal. It is evident that double integrator (2nd algorithm, left) has positive influence [8]. In the case of triangular or ramp reference signals, the asymptotic tracking of the 2nd algorithm can be expected against 1st algorithm, which always leads to steady-stare error (offset).

VII. CONCLUSION

Benefit of this paper consists in the compact solution of current limitation (subsection V.-B.), reliable filed weakening (subsection V.-A.) and in explicit predictive algorithms (section IV.). The solution is proved by experiments on developed PMSM drive prototype of rated power 10.7kW. The experiments confirmed simple implementation of the proposed algorithms and at least their same performance and computational demands as the conventional cascade vector PI control.

Fig. 6. Testing stand with PMSM drive.

TABLE I. PARAMETERS OF THE USED PMSM DRIVE

Symbol	Description	Value
P	rated power	10.7 kW
Uc	supply voltage	200 V
n_{max}	maximum speed	3000 rpm
R_s	stator resistance	0.28 Ω (Ohm)
L_s	stator inductance	0.003465 H (Henry)
ψ_M	PM rotor magnetic flux	0.1989 Wb (Weber)
B	viscous coef. of load	0 s^{-2}
p	number of pole pairs	4
J	moment of inertia	0.04 kg m^2
τ_L	load torque	0 N m

TABLE II. PARAMETERS OF THE 1ST GPC ALGORITHM

Symbol	Description	Value (A)	Value (B)
N	horizon of prediction	4	4
$\mathbf{Q}_{yw}$	output penalization	diag(2, 1, 2)	diag(10, 10, 30)
$\mathbf{Q}_{\Delta y}$	out. incr. penalization	diag(100, 20, 2)	diag(20, 80, 5)
$\mathbf{Q}_{\Delta u}$	input incr. penalization	diag(14, 7)	diag(5, 3.5)
Ts	sampling period	0.000125 s	0.000125 s
k_{fw}	field weakening gain	10^4	10^4
k_{iub}	margin coefficient	0.9	0.9
k_{sp}	current limitation exponent	40	40

TABLE III. PARAMETERS OF THE 2ND GPC ALGORITHM

Symbol	Description	Value (A)	Value (B)
N	horizon of prediction	4	4
$\mathbf{Q}_{yw}$	output penalization	diag(10, 5, 4)	diag(10, 5, 10)
$\mathbf{Q}_{\Delta y}$	out. incr. penalization	diag(140, 80, 1)	diag(20, 80, 1)
$\mathbf{Q}_{\Delta u}$	input incr. penalization	diag(20, 8)	diag(10, 8)
Ts	sampling period	0.000125 s	0.000125 s
k_{fw}	field weakening gain	4×10^4	4×10^4
k_{iub}	margin coefficient	0.9	0.9
k_{sp}	current limitation exponent	100	50

ACKNOWLEDGMENT

The paper was supported by the grant No. GP102/11/0437.

REFERENCES

[1] H. Liu and S. Li, "Speed Control for PMSM Servo System Using Predictive Functional Control and Extended State Observer". IEEE Trans. on Industrial Electronics, 2012, vol.59, no.2, pp. 1171-1183.

[2] L. Wang, Model Predictive Control System Design and Implementation Using MATLAB®, Springer, 2009.

[3] M. Preindl and S. Bolognani, "Model Predictive Direct Speed Control with Finite Control Set of PMSM Drive Systems", in IEEE Trans. on Power Electronics, 2013, vol.28, no.2, pp. 1007–1015.

[4] K. Belda and D. Vošmik, "Speed Control of PMSM Drives by Generalized Predictive Algorithms". Proc. of the 38th Conf. of the IEEE Industrial Electronics Society. ETS, Canada, 2012, pp. 2002-2007.

[5] A. Linder and R. Kennel, "Model Predictive Control for Electrical Drives", in IEEE Power Electronics Specialists Conf., 2005, pp. 1793-1799.

[6] K. Belda, "Study of Predictive Control for Permanent Magnet Synchronous Motor Drives. Proc. of the 17th IEEE Int. Conf. on Methods & Models in Automation and Robotics. WPU, Poland, 2012, pp. 522-527.

[7] K. Belda, "On Offset Free Generalized Predictive Control". Proc. of 19th Int. Conf. on Process Control. High Tatras, Slovak Republic, 2013, 6 pp.

[8] R. Wang, (2012-01-28). "Initial and Final Value Theorems". http://fourier.eng.hmc.edu/e102/lectures/Laplace_Transform/node17.html.

[9] E.J. Fuentes, C.A. Silva, and J.I. Yuz, "Predictive Speed Control of a Two-Mass System Driven by a Permanent Magnet Synchronous Motor". IEEE Trans. on Industrial Electronics, 2012 vol.59, no.7, pp. 2840-2848.

[10] J. Stumper, A. Dotlinger, J. Jung, and R. Kennel, "Predictive control of a PMSM based on real-time dynamic optimization". Proc. of the 14th European Conf. Electronics and Applications, 2011, pp. 1-8.